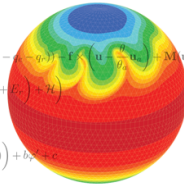


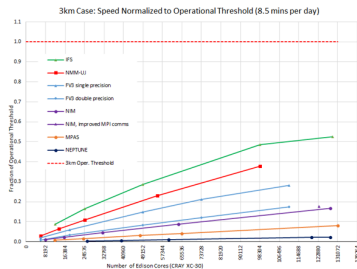
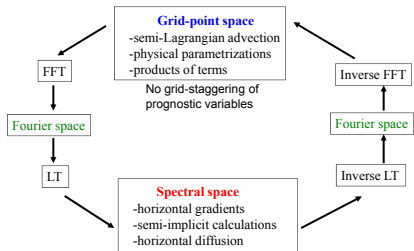
# Simulating all-scale global weather with the Finite-Volume Module of IFS

Christian Kühnlein, Sylvie Malardel, Piotr Smolarkiewicz, Nils Wedi

$$\begin{aligned}
 \frac{\partial \mathcal{G}\rho}{\partial t} + \nabla \cdot (\mathbf{v}\mathcal{G}\rho) &= 0 \\
 \frac{\partial \mathcal{G}\rho\mathbf{u}}{\partial t} + \nabla \cdot (\mathbf{v}\mathcal{G}\rho\mathbf{u}) &= \mathcal{G}\rho \left( -\Theta_d \tilde{\mathbf{G}} \nabla \varphi' - \frac{\mathbf{g}}{\theta_a} (\theta' + \theta_a (c q'_v - q'_r - q'_c)) + \mathbf{f} \cdot \left( \mathbf{u} + \frac{\mathbf{u}}{\theta_a} \right) + \mathbf{M}(\mathbf{u}) + \mathbf{D} \right) \\
 \frac{\partial \mathcal{G}\rho\theta'}{\partial t} + \nabla \cdot (\mathbf{v}\mathcal{G}\rho\theta') &= \mathcal{G}\rho \left( -\tilde{\mathbf{G}}^T \mathbf{u} \cdot \nabla \theta_a - \frac{L}{c_p \pi} \left( \frac{\Delta q_{\text{eva}}}{\Delta t} + L_c \right) + H \right) \\
 \frac{\partial \mathcal{G}\rho q_k}{\partial t} + \nabla \cdot (\mathbf{v}\mathcal{G}\rho q_k) &= \mathcal{G}\rho \mathcal{R}^{q_k} \\
 \frac{\partial \mathcal{G}\rho\varphi'}{\partial t} + \nabla \cdot (\mathbf{v}\mathcal{G}\rho\varphi') &= \mathcal{G}\rho \sum_{\ell=1}^3 \left( \frac{a_\ell}{\zeta_\ell} \nabla \cdot \zeta_\ell (\tilde{\mathbf{v}} - \tilde{\mathbf{G}}^T \mathbf{C} \nabla \varphi') \right) + b_\ell \varphi' + c
 \end{aligned}$$



Schematic of spectral-transform method in IFS



Current operational configuration of the Integrated Forecasting System (IFS) at the European Centre for Medium-Range Weather Forecasting:

- hydrostatic primitive equations (nonhydrostatic option available; see Benard et al. 2014)
  - hybrid  $\eta - p$  vertical coordinate (Simmons and Burridge, 1982)
  - spherical harmonics representation in horizontal (Wedi et al., 2013)
  - finite-element discretisation in vertical (Untch and Hortal, 2004)
  - semi-implicit semi-Lagrangian (SISL) integration scheme (Temperton et al. 2001, Diamantakis 2014)
  - cubic-octahedral ("TCo") grid (Wedi, 2014, Malardel et al. 2016)
  - HRES: TCo1279 (O1280) with  $\Delta_h \approx 9$  km and 137 vertical levels
  - ENS (1+50 perturbed members): TCo639 (O640) with  $\Delta_h \approx 16$  km and 91 vertical levels
- ⇒ ECMWF strategy for the year 2025 targets to run ENS with TCo1999 with  $\Delta_h \approx 5$  km

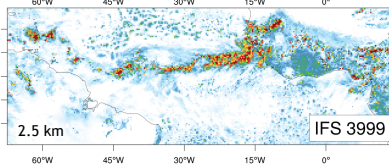
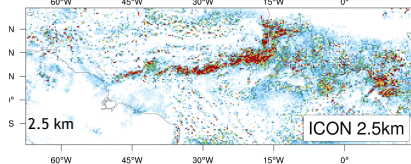
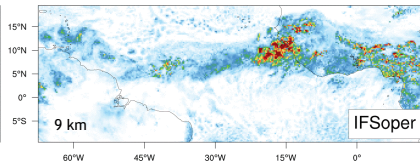
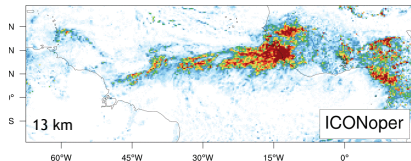
## Greyzone evaluations

*Daniel Klocke and Nils Wedi*

1, 2.5, 5, ~9 km of Tropical Atlantic with ICON & IFS

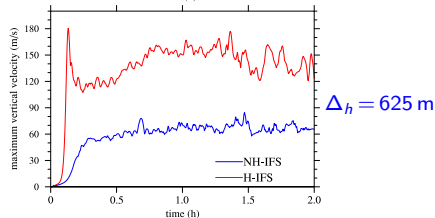
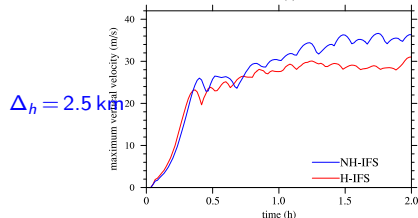
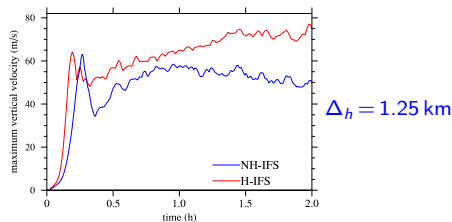
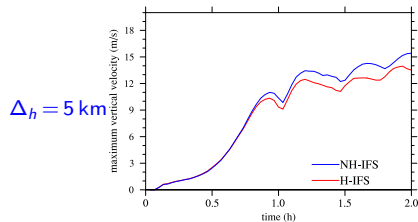
tqc 2016081100 +13h

Total water + ice content



# Quasi-hydrostatic versus nonhydrostatic dynamics

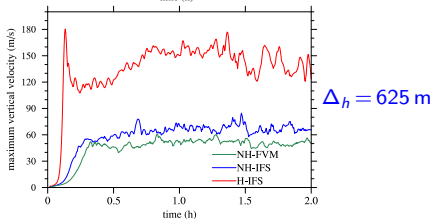
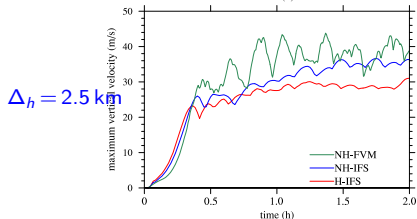
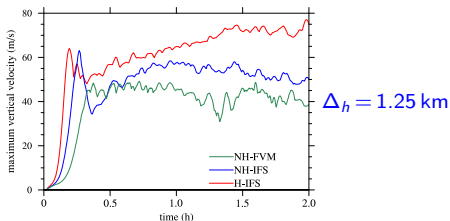
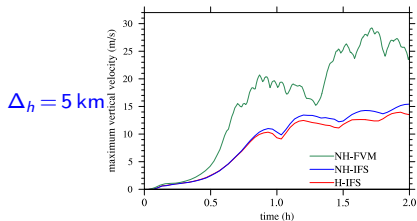
Idealized convective storm (Klemp et al. 2015) on a small planet (1/25 reduced) with H and NH formulation of IFS: From what horizontal grid spacing  $\Delta_h$  appear significant differences?



→ H-IFS and NH-IFS use Forbes et al. 2011 microphysics and similar numerical configurations, in particular TCo grid, FD in vertical, ICI, no explicit diffusion, no convection scheme)

# Quasi-hydrostatic versus nonhydrostatic dynamics

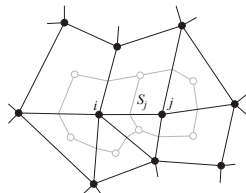
Idealized convective storm (Klemp et al. 2015) on a small planet (1/25 reduced) with H and NH formulation of IFS and NH-FVM:



→NH-FVM uses smaller time steps and different microphysics parametrisation!

# Finite-Volume Module (FVM) of IFS—key formulation features

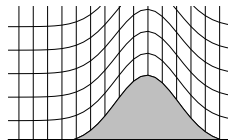
- deep-atmosphere nonhydrostatic Euler equations in geospherical framework (Szmelter and Smolarkiewicz 2010; Smolarkiewicz et al. 2016; Smolarkiewicz, Kühnlein, Grabowski 2017; Kühnlein, Malardel, Smolarkiewicz *in prep.*)
- flexible height-based terrain-following vertical coordinate
- hybrid of horizontally-unstructured median-dual finite-volume with vertically-structured finite-difference/finite-volume discretisation (Szmelter and Smolarkiewicz 2010; Smolarkiewicz et al. 2016)
- all prognostic variables are co-located
- two-time-level semi-implicit integration scheme with 3D implicit acoustic, buoyant and rotational modes (Smolarkiewicz, Kühnlein, Wedi JCP 2014)
- preconditioned generalised conjugate residual iterative solver for 3D elliptic problems arising in the semi-implicit integration schemes (Smolarkiewicz and Szmelter 2011 for a more recent review)
- non-oscillatory finite-volume MPDATA scheme (Smolarkiewicz and Szmelter 2005; Kühnlein and Smolarkiewicz 2017)
- octahedral reduced Gaussian grid, but the FVM formulation not restricted to this (Szmelter and Smolarkiewicz 2016)
- optional moving mesh capability (as in Kühnlein, Smolarkiewicz, Dörnbrack 2012)



median-dual finite-volume approach

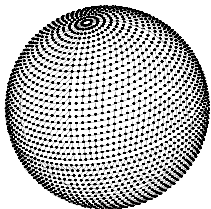
$$\int_{\Omega} \nabla \cdot \mathbf{A} = \int_{\partial\Omega} \mathbf{A} \cdot \mathbf{n} = \frac{1}{V_i} \sum_{j=1}^{l(i)} A_j^{\perp} S_j$$

dual volume:  $V_i$ , face area:  $S_j$

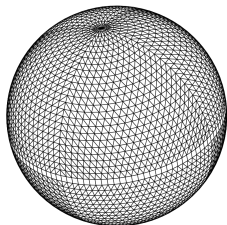
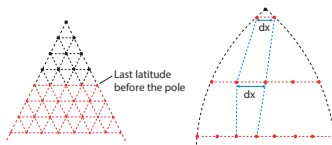
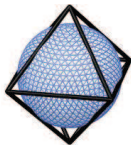


terrain-following coordinate

# Octahedral reduced Gaussian grid



Nodes of octahedral grid 'O24'



Primary mesh about nodes of octahedral grid in FVM

- octahedral reduced Gaussian grid (*octahedral grid* of size  $O_X$ )
  - suitable for spherical harmonics transforms applied in spectral IFS
    - Gaussian latitudes  $\Rightarrow$  Legendre transforms
    - equidistant distribution of nodes along latitudes following octahedral rule  $\Rightarrow$  Fourier transforms
  - FVM develops median-dual mesh around nodes of octahedral grid
- $\Rightarrow$  finite-volume and spectral-transform IFS can operate on same quasi-uniform horizontal grid
- $\rightarrow$  Malardel et al. ECMWF Newsletter 2016, Smolarkiewicz et al. JCP 2016
- $\rightarrow$  operational at ECMWF with HRES and ENS since March 2016
- [Mesh generator and parallel data structures for FVM provided by ECMWF's Atlas framework \(Deconinck et al. 2017\)](#)

Flux-form moist compressible Euler equations in generalised curvilinear coordinates (Smolarkiewicz, Kühnlein, Grabowski 2017; Kühnlein, Malardel, Smolarkiewicz *in prep.*):

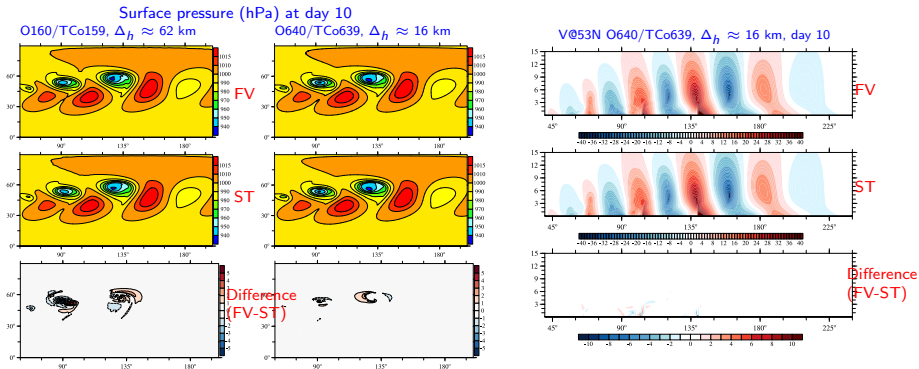
$$\begin{aligned} \frac{\partial \mathcal{G} \rho_d}{\partial t} + \nabla \cdot (\mathbf{v} \mathcal{G} \rho_d) &= 0, \\ \frac{\partial \mathcal{G} \rho_d \mathbf{u}}{\partial t} + \nabla \cdot (\mathbf{v} \mathcal{G} \rho_d \mathbf{u}) &= \mathcal{G} \rho_d \left[ -\theta_\rho \tilde{\mathbf{G}} \nabla \varphi' + \mathbf{g} \mathcal{B} - \mathbf{f} \times \left( \mathbf{u} - \frac{\theta_\rho}{\theta_{\rho a}} \mathbf{u}_a \right) + \mathcal{M}' + \mathcal{D} + \mathbf{P}^u \right], \\ \frac{\partial \mathcal{G} \rho_d \theta'}{\partial t} + \nabla \cdot (\mathbf{v} \mathcal{G} \rho_d \theta') &= \mathcal{G} \rho_d \left[ -\tilde{\mathbf{G}}^T \mathbf{u} \cdot \nabla \theta_a + \mathcal{H} + P^{\theta'} \right], \\ \frac{\partial \mathcal{G} \rho_d r_k}{\partial t} + \nabla \cdot (\mathbf{v} \mathcal{G} \rho_d r_k) &= \mathcal{G} \rho_d [\mathcal{D}^{rk} + P^{rk}] \quad \text{where } r_k = r_v, r_c, r_r, r_i, r_s, \\ \varphi' &= c_{pd} \left[ \left( \frac{R_d}{\rho_0} \rho_d \theta (1 + r_v/\varepsilon) \right)^{R_d/c_{vd}} - \pi_a \right], \end{aligned}$$

with:

$$\begin{aligned} \mathbf{v} &= \tilde{\mathbf{G}}^T \mathbf{u}, \quad \theta_\rho = \frac{\theta (1 + r_v/\varepsilon)}{(1 + r_t)}, \quad \varepsilon = \frac{R_d}{R_v}, \quad \theta' = \theta - \theta_a, \\ \mathcal{B} &= 1 - \frac{\theta_\rho}{\theta_{\rho a}} = 1 - \frac{\eta \theta_\rho}{\theta_a + \theta'}, \quad \eta \theta_\rho \equiv \frac{1 + r_v/\varepsilon}{1 + r_t}, \quad r_t = \sum_k r_k \end{aligned}$$

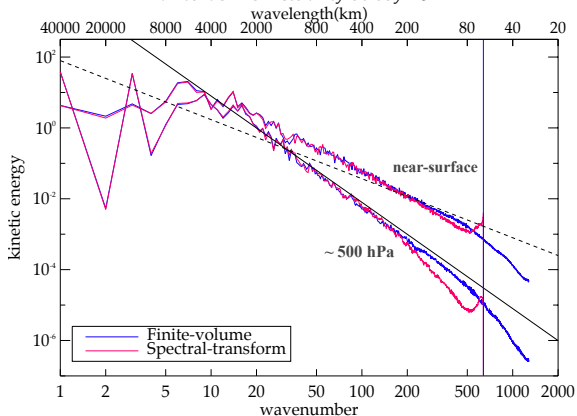


Dry baroclinic instability (Ullrich et al. 2014) with FVM and spectral-transform IFS (ST):



- Finite-volume solutions achieve accuracy of established spectral-transform IFS for planetary-scale baroclinic instability

*Instantaneous kinetic energy spectra O640/TCo639 ( $\Delta_h \approx 16$  km)  
for baroclinic instability at day 15*

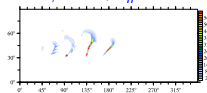


# Finite-volume and spectral-transform solutions in IFS

Moist baroclinic instability with FVM and spectral-transform IFS (ST) with large-scale condensation and diagnostic precipitation:

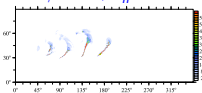
Precipitation (mm/day) at day 10

O160/TCo159,  $\Delta_h \approx 62$  km



FV

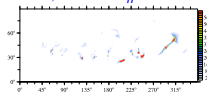
O640/TCo639,  $\Delta_h \approx 18$  km



ST

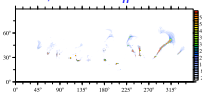
Precipitation (mm/day) at day 15

O160/TCo159,  $\Delta_h \approx 62$  km



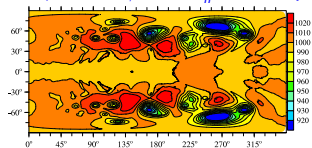
FV

O640/TCo639,  $\Delta_h \approx 18$  km

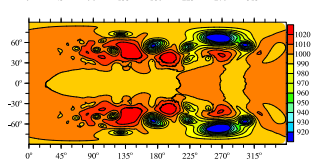


ST

Surface pressure O640/TCo639,  $\Delta_h \approx 18$  km, day 15



FV



ST

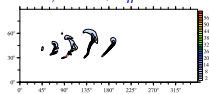
- Finite-volume solutions achieve accuracy of established spectral-transform IFS for moist flows

# Finite-volume and spectral-transform solutions in IFS

Moist baroclinic instability with FVM and spectral-transform IFS (ST) with large-scale condensation and diagnostic precipitation:

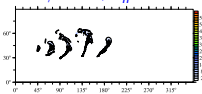
Precipitation (mm/day) at day 10

O160/TCo159,  $\Delta_h \approx 62$  km



FV

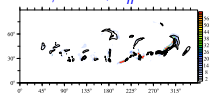
O640/TCo639,  $\Delta_h \approx 18$  km



ST

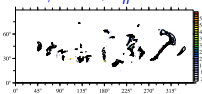
Precipitation (mm/day) at day 15

O160/TCo159,  $\Delta_h \approx 62$  km



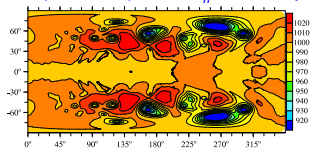
FV

O640/TCo639,  $\Delta_h \approx 18$  km

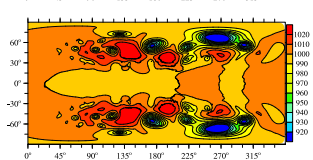


ST

Surface pressure O640/TCo639,  $\Delta_h \approx 18$  km, day 15



FV

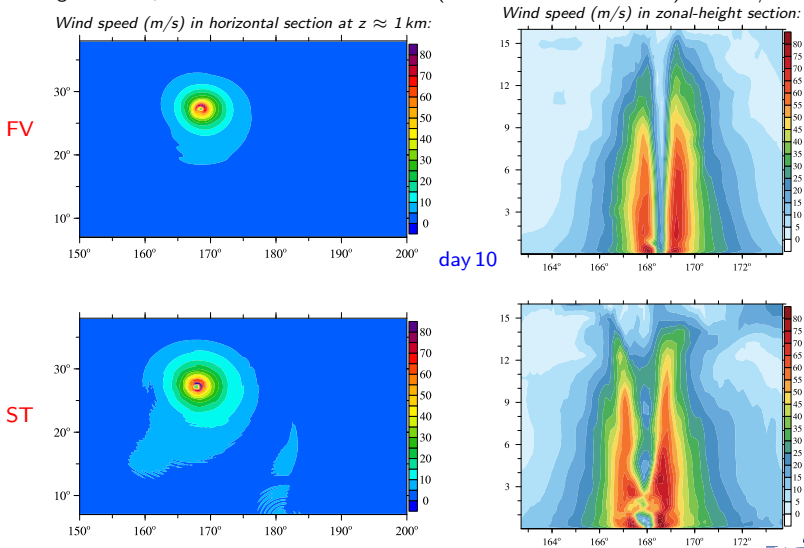


ST

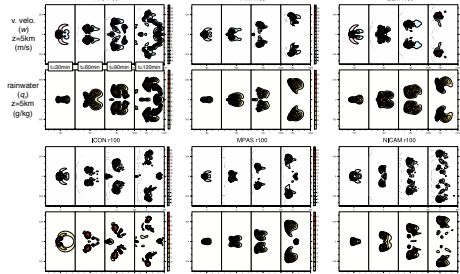
- Finite-volume solutions achieve accuracy of established spectral-transform IFS for moist flows

# Tropical cyclone simulations with FV and ST approaches in IFS

Tropical cyclone simulations with coupling to parametrisations for large-scale condensation with diagnostic rain, surface fluxes and PBL diffusion (Reed and Jablonowski 2011) on O640/L60:



## Time evolution of supercells at 1km resolution



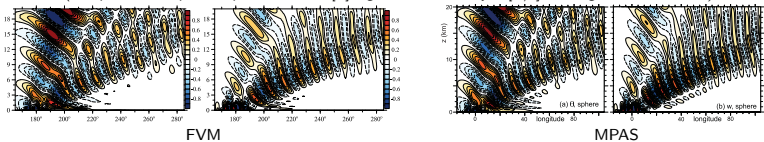
Geosci. Model Dev. Discuss., <https://doi.org/10.5194/gmd-2017-108>  
 Manuscript under review for journal Geosci. Model Dev.  
 Discussion started 6 June 2017  
 © Author(s) 2017. CC BY 3.0 License.



## DCMIP2016: A Review of Non-hydrostatic Dynamical Core Design and Intercomparison of Participating Models

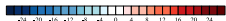
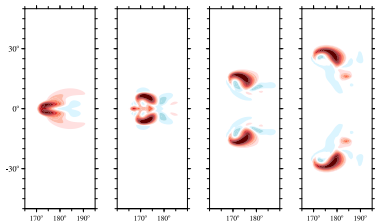
Paul A. Ullrich<sup>1</sup>, Christiane Jablonowski<sup>2</sup>, James Keen<sup>3</sup>, Peter H. Lauritzen<sup>4</sup>, Ramachandran Nair<sup>4</sup>, Kevin A. Riene<sup>5</sup>, Colin M. Zarzycki<sup>6</sup>, David M. Hall<sup>7</sup>, Don Darkich<sup>8</sup>, Ross Heikes<sup>9</sup>, Cédric Kommer<sup>10</sup>, David Randall<sup>11</sup>, Thomas Dunne<sup>12</sup>, Yann Ménelou<sup>13</sup>, Xi Chen<sup>14</sup>, Lucas Harter<sup>15</sup>, Christian Köhler<sup>16</sup>, Vivian Lee<sup>17</sup>, Abdesamad Qadiri<sup>18</sup>, Claude Girard<sup>19</sup>, Marco Giogetta<sup>20</sup>, Daniel Reintz<sup>21</sup>, Joseph Klemp<sup>22</sup>, Sang-Hun Park<sup>23</sup>, William Skamarock<sup>24</sup>, Hiroaki Miura<sup>25</sup>, Tomoki Ohno<sup>26</sup>, Ryopu Yoshida<sup>27</sup>, Robert Walco<sup>28</sup>, Alex Reinecke<sup>29</sup>, and Kevin Vittori<sup>30</sup>

FVM and MPAS results for stratified flow past Schär mountain on a reduced-radius planet after 2 h  
 (left: potential temperature perturbation  $\theta'$  [K], right: vertical velocity  $w$  [m/s], lon-height section at lat=0)

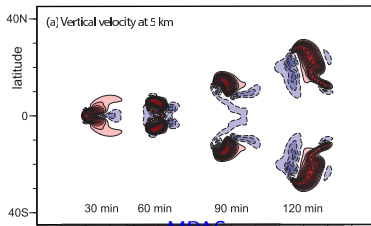
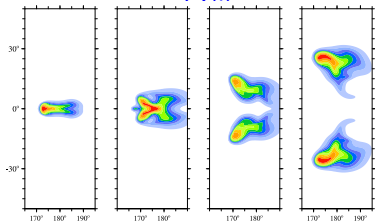


# Mesoscale convective storm on reduced-size planet

Supercell evolution (0.5, 1, 1.5, 2h) with FVM (left) and MPAS (right) at  $\approx 0.5$  km grid spacing (cf. Klemp et al. 2015):

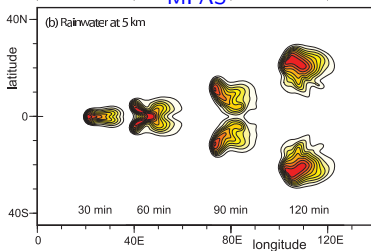


FVM



MPAS

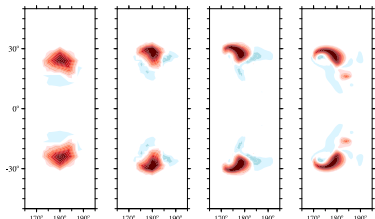
Vertical velocity (m/s) at 5 km



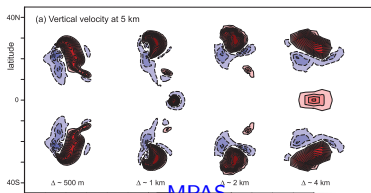
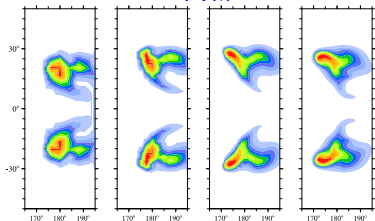
Rainwater (g/kg) at 5 km

# Mesoscale convective storm on reduced-size planet

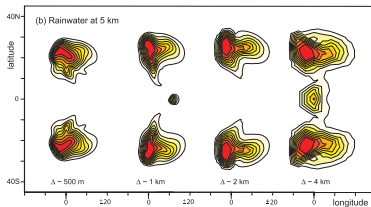
Supercell for grid spacings (4, 2, 1, 0.5 km) with FVM (left) and MPAS (right) after 2 h of simulation (cf. Klemp et al. 2015):



FVM



Vertical velocity (m/s) at 5 km



Rainwater (g/kg) at 5 km



## Further reading:

- Kühnlein C., P. K. Smolarkiewicz, A. Dörnbrack, Modelling atmospheric flows with adaptive moving meshes., *J. Comput. Phys.*, 2012.
- Szmelter J., P. K. Smolarkiewicz P.K, An edge-based unstructured mesh discretisation in a geospherical framework., *J. Comput. Phys.*, 2010.
- Smolarkiewicz P.K., C. Kühnlein, N. P. Wedi, A discrete framework for consistent integrations of soundproof and compressible PDEs of atmospheric dynamics., *J. Comput. Phys.*, 2014.
- Smolarkiewicz P.K., W. Deconinck, M. Hamrud, C. Kühnlein, G. Modzinski, J. Szmelter, N. P. Wedi, A finite-volume module for simulating global all-scale atmospheric flows., *J. Comput. Phys.*, 2016.
- Kühnlein C., Smolarkiewicz P.K., An unstructured-mesh finite-volume MPDATA for compressible atmospheric dynamics., *J. Comput. Phys.*, 2017.
- Smolarkiewicz P.K., C. Kühnlein, W. W. Grabowski, A finite-volume module for cloud-resolving simulations of global all-scale atmospheric flows., *J. Comput. Phys.*, 2017.
- Deconinck W., P. Bauer, M. Diamantakis, M. Hamrud, C. Kühnlein, G. Mengaldo, P. Marciel, T. Quintino, B. Raoult, P. K. Smolarkiewicz, N. P. Wedi, *Atlas: The ECMWF framework to flexible numerical weather and climate modelling.*, <https://doi.org/10.1016/j.cpc.2017.07.006>, 2017.
- Waruszewski M., C. Kühnlein, H. Pawlowska, P. K. Smolarkiewicz, MPDATA: Third-order accuracy for arbitrary flows, *in press, JCP*.
- Smolarkiewicz P.K., C. Kühnlein, N. P. Wedi, Perturbation equations for all-scale atmospheric dynamics., *submitted to J. Comput. Phys.*
- Kühnlein C., S. Malardel, Smolarkiewicz P.K., et al., Finite-volume and spectral-transform solutions in IFS, *in preparation for GMD*
- Kühnlein C., R. Klein, Smolarkiewicz P.K., Splitting of advection in an all-scale atmospheric model, *in preparation for MWR*